

Mini-ring approach for high-throughput drug screenings in 3D tumor models

Nhan Phan^{1,2}, Bobby Tofig³, Deanna M. Janzen⁴, Jin Huang⁴, Sanaz Memarzadeh⁴⁻⁸, Robert Damoiseaux^{3,9} and Alice Soragni^{1,8*}

¹Division of Hematology-Oncology, Department of Medicine, David Geffen School of Medicine, University of California Los Angeles, CA, 90095

²Laboratory of Stem Cell Research and Application, University of Science, Vietnam National University, HCM City, Vietnam

³Molecular Screening Shared Resource, California NanoSystems Institute, University of California Los Angeles, CA 90095

⁴Department of Obstetrics and Gynecology, David Geffen School of Medicine, University of California Los Angeles, CA, 90095

⁵Eli and Edythe Broad Center of Regenerative Medicine and Stem Cell Research, University of California Los Angeles, CA 90095

⁶The VA Greater Los Angeles Health Care System, Los Angeles, CA, 90073

⁷Department of Biological Chemistry, University of California Los Angeles, CA 90095

⁸Molecular Biology Institute, University of California Los Angeles, CA 90095

⁹Department of Molecular and Medicinal Pharmacology, David Geffen School of Medicine, University of California Los Angeles, CA, 90095

* Correspondence to AS (alices@mednet.ucla.edu)

Abstract

There is increasing interest in developing 3D tumor organoid models for drug development and personalized medicine applications. While tumor organoids are in principle amenable to high-throughput drug screenings, progress has been hampered by technical constraints and extensive manipulations required by current methodologies. Here, we introduce a miniaturized, fully automatable, flexible high-throughput method using a simplified geometry to establish 3D organoids from cell lines and primary tissue and robustly assay drug responses.

Introduction

Preclinical drug development and discovery has relied heavily on traditional 2D cell culture methods. Nevertheless, 3D cancer models are a better approximation of the tumor of origin in terms of cell differentiation, microenvironment, histoarchitecture and drug response¹⁻⁸. Various methods to set up tumor spheroids or organoids have been proposed, including using low-attachment U-bottom plates, feeding layers or various biological and artificial matrices^{2,5,6,9-15}. Methods using low-attachment U-bottom plates ideally only carry one organoid per well, have limited automation and final assay capabilities¹¹⁻¹³. In addition, not all cells are capable of forming organized 3D structures with this method. Approaches that include a bio-matrix, such as Matrigel, have the potential to offer a scalable alternative in which cancer cells thrive^{2,7,16,17}. However, several approaches so far rely on thick volumes of matrix which is not cost-effective, potentially hard for drugs to efficiently penetrate and difficult to dissolve fully at the end of the experiment¹⁶. In other applications, organoids are first formed and then transferred to different plates for drug treatment or final readout which can result in the tumor spheres sticking to plastic or breaking^{7,17}. In addition, some assays require to disrupt the organoids to single cell suspensions at the end of the experiment^{9,15}. All of these manipulations introduce significant variability limiting applicability in screening efforts⁵. To overcome these limitations, we optimized an assay system for 3D organoid high-throughput drug screenings that takes advantage of a specific geometry. Our miniaturized ring methodology does not require functionalized plates. Organoids are assayed in the same plate where they are seeded, with no need for sample transfer at any stage or dissociation of the pre-formed tumor organoids to single cell suspensions. Here we show that the mini-ring approach is simple, robust, requires few cells and can be easily automated for high-throughput applications.

Results and Discussion

Single cell suspensions are pre-mixed with cold Matrigel (3:4 ratio) and 10 μ l of this mixture is plated in a ring shape around the rim of the wells of a 96 well plate (**Fig. 1a**). The Matrigel rapidly solidifies upon short incubation at 37°C (**Fig. 1a**). The combination of small volume and surface tension holds the cells in place until the Matrigel solidifies and prevents 2D growth at the center of the wells. This configuration allows further media removal, changes of conditions or treatment addition to be easily performed by pipetting in the center of the well, preventing any disruption of the gel. Cancer cell lines grown in the mini-ring format give rise to organized tumor organoids that recapitulate features of the original histology (**Fig 1b and S1; Table S1**). The mini-ring approach is also suitable to establish patient-derived tumor organoids (PDTOs). Primary patient samples grow and maintain the heterogeneity of the original tumor as expected. As an example, Patient #1 PDTOs recapitulate features of high-grade serous carcinoma (HGSC) as well as clear cell tumor (**Fig. 1b**). Fewer than 5000 cells per well are sufficient to provide a quantifiable readout (**Fig. 1b**).

Next, we optimized a treatment protocol and readouts for the mini-ring approach. Our standardized paradigm includes: seeding cells on day 0, establishing organoids for 2-3 days followed by two consecutive daily treatments, each performed by complete medium change (**Fig. 1c**). Three drugs (ReACp53⁹, Staurosporine and Doxorubicin) were tested at five concentrations in triplicates (**Fig. 1d-g**). We optimized different readouts in order to adapt the method to a specific research question or instrument availability. After seeding cells in standard white plates, we

performed a luminescence-based ATP assay to obtain a metabolic readout of cell status, calculate EC₅₀ and identify cell-specific sensitivities (**Fig. 1, S2 and S3**). Results show how the Matrigel in the mini-ring setup is thin enough to allow penetration not only of small molecules but also of higher molecular weight biologics such as peptides⁹. We performed two consecutive treatments which allows the drugs to not only penetrate the gel but also to reach organoids that may be bulky⁹. However, the assay is flexible and can be easily adapted to single treatments followed by longer incubations, multiple consecutive recurring treatments, multi-drug combinations or other screening strategies (**Fig. S3**).

We also implemented assays to quantify drug response by measuring cell viability after staining of live organoids with specific dyes followed by imaging. We optimized a calcein-release assay coupled to propidium iodide (PI) staining and a caspase 3/7 cleavage assay (**Fig. 1e-g and S4**). Both are performed after seeding the cells in standard black plates. Tumor organoids are stained with the reagents after dispase release and neutralization. After a 30-45 minute incubation, organoids are imaged with a Celigo S cell imager. Images are then segmented and quantified (**Fig. 1e-g and S4**). As the organoids are assayed in the same well in which they are seeded, it is important to determine which assay/plate to use beforehand. Although the assays are testing different biological events, results are concordant across the methods for the three molecules we tested (**Fig. 1, S4 and S5**).

Precision medicine approaches to cancer therapy almost exclusively rely on genomics¹⁸. However, recent data shows that only a small percentage of patients has benefited from tumor sequencing so far¹⁸⁻²⁰. A rapid functional assay to determine drug sensitivities of primary specimens can offer actionable information to help tailoring therapy to individual cancer patients¹⁸. We tested suitability of our approach to rapidly and effectively identify drug susceptibilities of primary ovarian cancer samples obtained from the operating room. We used one patient-derived cell line, S1 GODL²¹, to optimize conditions (**Fig. S5**) and two ovarian cancer patient samples as test cases (**Table S1 and Fig. 2**).

In order to maximize the amount of information extracted from irreplaceable clinical samples, we investigated the possibility to concurrently perform multiple assays on the same plate. We optimized the initial seeding cell number (5000 cells/well) to couple the ATP metabolic assay to 3D tumor count and total organoid area measurement. This seeding density yields a low-enough number of organoids to facilitate size distribution analysis but sufficient ATP signal to be within the dynamic range of the CaspaseGlo 3D assay. We prepared six 96 well plates and tested 252 different kinase inhibitors at two different concentrations for each patient (120 nM and 1 μ M). We used the same experimental paradigm optimized above. All steps (media change, drug treatment) were automated and performed in less than 2 minutes/plate using a Beckman Coulter Biomek FX integrated into a Thermo Spinnaker robotic system. At the end of the experiment, PDOs were first imaged in brightfield mode for organoid count/size distribution analysis followed by the ATP assay. The two measurements yielded high quality data that converged on several hits, highlighting the feasibility of our approach (**Fig. 2a and c**). The three samples tested showed minimal overlap in their response to kinase inhibitors thus the assay unmasked individual sensitivities to different drugs (**Fig. 2a-g**).

Cells obtained from Patient #1 at the time of cytoreductive surgery²¹ were chemo-naïve, and the heterogeneous nature of this clear cell/HGSC tumor was fully recapitulated in the PDOs (**Fig. 1b**). The organoids were sensitive to 16/252 molecules tested and responded mostly to a variety of cyclin-dependent kinase (CDK) inhibitors with a stronger response to inhibitors hitting CDK1/2 in combination with CDK 4/6 or CDK 5/9 (**Fig. 2a-c and S5b**). Interestingly, CDK inhibitors have found limited applicability in ovarian cancer therapy so far²².

Based on the profiles of the CDK inhibitors tested and on the response observed (**Fig. S5b-c**), we selected four untested molecules to assay. We anticipated that Patient #1 should not respond to Palbociclib (targeting only CDK4/6) and THZ1 (CDK7) while expecting a response to JNJ-7706621 (CDK1/2/3/4/6) and AZD54338 (CDK1/2/9; **Fig. S5b-**

c). However, we observed a strong response to THZ1 (**Fig. 2h**). Both THZ1 and BS-181 HCl specifically target CDK7. Nevertheless, Patient #1 PDOs showed a strong response to the former but no response to the latter which could be attributed to the different activity of the two as recently observed in breast cancer²³.

Cells were obtained from Patient #2, a heavily pre-treated patient diagnosed with progressive, platinum-resistant HGSC (**Table S1**). PDOs showed a strong response to only 3/252 drugs tested, with sensitivity to two of these (BGT226, a PI3K/mTOR inhibitor and Degrasyn, a deubiquitinases inhibitor) shared with all other tested samples (**Fig. 2c, 2f and S5a**). Moderate responses (50-60% residual cell viability at 1 μ M) were observed for EGFR inhibitors and we could detect high expression of EGFR at the plasma membrane of the tumor cells (**Fig. S5e**). Remarkably, Patient #2 PDOs showed a very moderate response to our positive control, Staurosporine, a pan-kinase inhibitor with very broad activity²⁴. The significant lack of response to multiple therapies observed for Patient #2 could be due to over-expression of efflux membrane proteins. Indeed, the PDOs showed a high level of expression of ABCB1 (**Fig. 2i**). High expression of the ATP-dependent detox protein ABCB1 is frequently found in chemoresistant ovarian cancer cells and recurrent ovarian cancer patients' samples and has been correlated with poor prognosis^{25,26}.

In conclusion, the mini-ring approach can be a robust tool to standardize precision medicine efforts¹⁸, given its ease of applicability to many different systems and drug screening protocols, as well as its limited cell requirement which allows testing of samples as obtained from biopsies/surgical specimens without the need for expansion. As demonstrated above, the method rapidly allowed us to pinpoint individual drug sensitivities and identify a tumor "fingerprint", with multiple inhibitors converging on a given pathway. Interestingly, many of the drugs identified in our screening do not have a specific, unequivocal biomarker or genomic signature predictive of response. Thus, patients may greatly benefit from PDO testing prior to therapy selection^{5,7,18,27}.

Our strategy can be successfully used to test patient samples that are recalcitrant to grow as patient-derived xenografts (PDX) *in vivo*. In fact, Patient #1 cells injected in NSG mice (500K/mouse, 12 mice) did not give rise to detectable tumor masses over six weeks (data not shown). While we apply the mini-ring setup to drug screenings, the same methodology is suitable for studies aiming at characterizing organoids' biological and functional properties with high throughput. Complete automation, scalability to 384 well plates, and flexibility to use different supports beside Matrigel can further extend applicability of the mini-ring approach.

Figures:

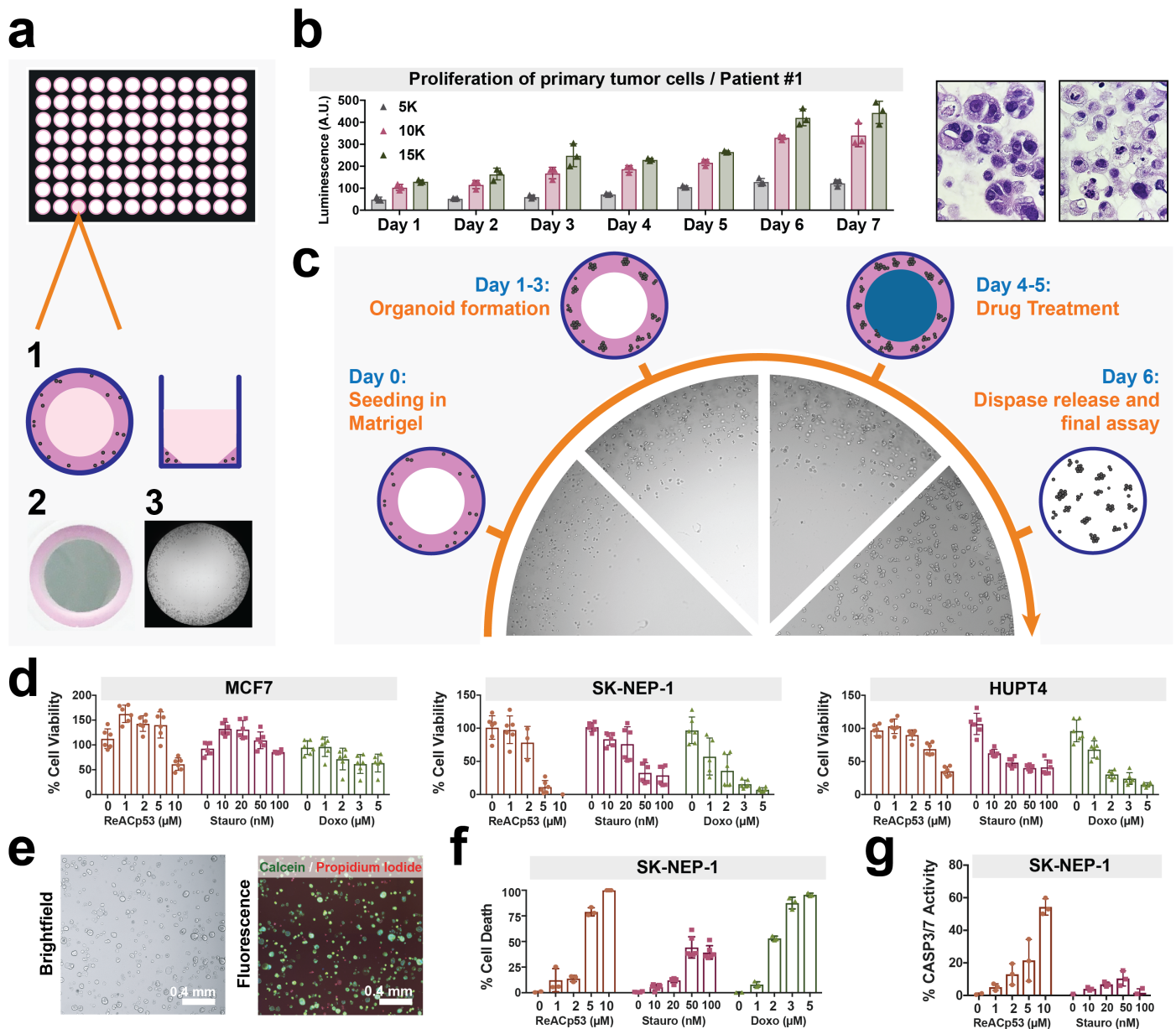


Figure 1. The mini-ring method for 3D tumor cell biology. (a) Schematics of the mini-ring setup. Cells are plated in Matrigel around the rim of the wells form a solid thin ring as depicted in 1 and photographed in 2, which has decreasing thickness. The picture in 3 acquired with a cell imager shows tumor organoids growing at the periphery of the well as desired, with no invasion of the center. (b) Proliferation of primary tumor cells as measured by ATP release. Different seeding densities were tested and compared (5, 10 and 15K cells). The mini-ring method allowed the patient sample to grow and maintain the heterogeneity and histology of the original ovarian tumor which had a high-grade serous carcinoma component (H&E left picture) and a clear cell component (H&E right picture). (c) Schematic of the drug-treatment experiments performed in the mini-ring setting. The pictures are representative images as acquired using a Celigo cell imager. (d - g) Assays to monitor drug response of cell lines using the mini-ring configuration. Three drugs (ReACp53, Staurosporine and Doxorubicin) were tested at five concentrations in triplicates for all cell lines. (d) ATP release assay (CellTiter-Glo 3D) readout. (e) and (f) Calcein/PI readout. (e) Representative image showing staining of MCF7 cells with the dyes and segmentation to quantify the different populations (live / dead). (f) Quantification of Calcein/PI assay for three-drug assay. (g) Quantification of cleaved caspase 3/7 assay. Doxorubicin was omitted due to its fluorescence overlapping with the caspase signal. For all graphs, symbols are individual replicates, bars represent the average and error bars show SD.

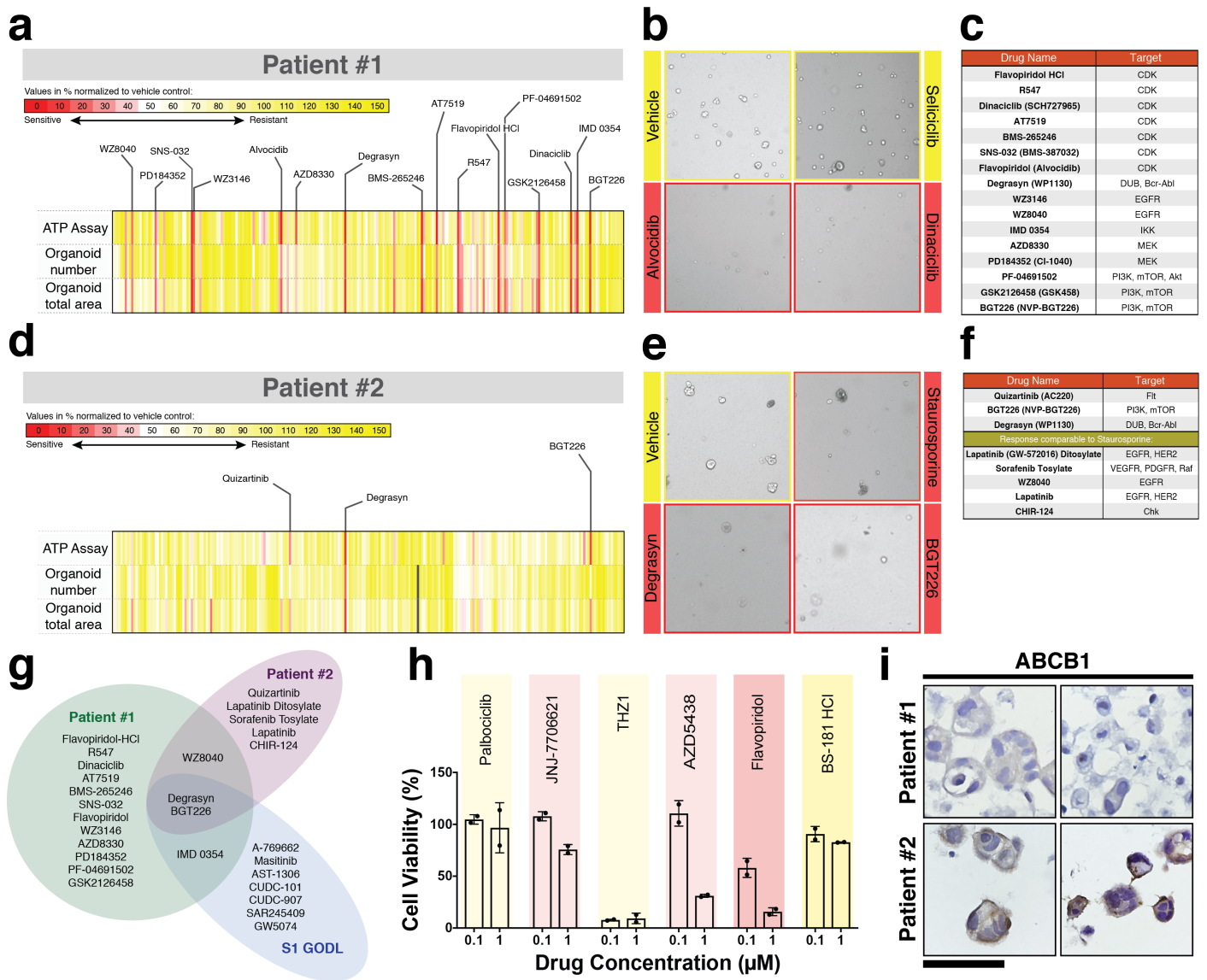


Figure 2. Mini-ring approach to unveil drug response patterns in PDTOs. (a) and (d) Results of kinase screening experiment. Two readouts were used for this assay: ATP quantification as measured by CellTiter-Glo 3D and organoids quantification evaluated by brightfield imaging. Brightfield images were segmented and quantified using the Celigo S Imaging Cell Cytometer Software. Both organoid number as well as total area were evaluated for their ability to capture response to drugs. In this plot, each vertical line is one drug, all 252 tested are shown. Values are normalized to the respective vehicle controls for each method and expressed as %. (b) and (e) A representative image of the effects of the indicated drug treatments as visualized by the Celigo cell imager. (c) and (f) Table of drug leads causing $\geq 75\%$ cell death. For Patient #2, we included drugs inducing a response comparable to the Staurosporine control ($\sim 60\%$ cell death). (g) Diagram illustrating limited overlap between the detected patterns of response identified through the mini-ring assay for Patients #1 and #2 and for the patient-derive line S1 GODL. (h) Small scale kinase assay on Patient #1 primary cells. ATP readout. Four molecules not present in the high-content screening were tested. We included two previously tested drugs, Flavopiridol and BS-181 HCl, as positive and negative control respectively. (i) Expression of the multi-drug efflux protein ABCB1 in PDTOs as visualized by IHC. Patient #2 expresses very high levels of the ABC transporter. Scale bar: $60 \mu\text{m}$.

Acknowledgments

We thank Dr. Dylan Conklin (UCLA) and Dr. David Eisenberg (UCLA) for helpful discussions and inputs and the Translational Oncology Research Labs at UCLA for donating most cell lines. This project was supported by a Worldwide Cancer Research grant to AS (#16-0253). We acknowledge support by the Hirshberg Foundation (to AS), the UCLA SPORE in Prostate Cancer (NIH P50CA092131, PI: Robert Reiter) and a Jonsson Cancer Center Foundation Impact Award (to SM).

Author Contributions

AS and NP designed the project and carried out the experiments. SM and DJ obtained, characterized and isolated the primary patient samples. JH contributed to feasibility experiments. BT and RB generated the kinase inhibitor drug library and optimized automation for primary sample assays. AS analyzed the data and wrote the paper with contributions from all authors.

References

1. Pickl, M. & Ries, C. H. Comparison of 3D and 2D tumor models reveals enhanced HER2 activation in 3D associated with an increased response to trastuzumab. *Oncogene* **28**, 461–468 (2008).
2. Katt, M. E., Placone, A. L., Wong, A. D., Xu, Z. S. & Searson, P. C. In Vitro Tumor Models: Advantages, Disadvantages, Variables, and Selecting the Right Platform. *Front. Bioeng. Biotechnol.* **4**, (2016).
3. Tanner, K. & Gottesman, M. M. Beyond 3D culture models of cancer. *Sci. Transl. Med.* **7**, 283ps9 (2015).
4. Nyga, A., Cheema, U. & Loizidou, M. 3D tumour models: novel in vitro approaches to cancer studies. *J. Cell Commun. Signal.* **5**, 239–248 (2011).
5. Fong, S., Debs, R. J. & Desprez, P.-Y. Id genes and proteins as promising targets in cancer therapy. *Trends Mol. Med.* **10**, 387–392 (2004).
6. Kimlin, L. C., Casagrande, G. & Virador, V. M. In vitro three-dimensional (3D) models in cancer research: an update. *Mol. Carcinog.* **52**, 167–182 (2013).
7. Pauli, C. *et al.* Personalized In Vitro and In Vivo Cancer Models to Guide Precision Medicine. *Cancer Discov.* **7**, 462–477 (2017).
8. Halfter, K. & Mayer, B. Bringing 3D tumor models to the clinic - predictive value for personalized medicine. *Biotechnol. J.* **12**, (2017).
9. Soragni, A. *et al.* A Designed Inhibitor of p53 Aggregation Rescues p53 Tumor Suppression in Ovarian Carcinomas. *Cancer Cell* **29**, 90–103 (2016).
10. Breslin, S. & O'Driscoll, L. Three-dimensional cell culture: the missing link in drug discovery. *Drug Discov. Today* **18**, 240–249 (2013).
11. Breslin, S. & O'Driscoll, L. The relevance of using 3D cell cultures, in addition to 2D monolayer cultures, when evaluating breast cancer drug sensitivity and resistance. *Oncotarget* **7**, 45745–45756 (2016).

12. Friedrich, J., Seidel, C., Ebner, R. & Kunz-Schughart, L. A. Spheroid-based drug screen: considerations and practical approach. *Nat. Protoc.* **4**, 309–324 (2009).
13. Zaroni, M. *et al.* 3D tumor spheroid models for in vitro therapeutic screening: a systematic approach to enhance the biological relevance of data obtained. *Sci. Rep.* **6**, 19103 (2016).
14. Kelm, J. M., Timmins, N. E., Brown, C. J., Fussenegger, M. & Nielsen, L. K. Method for generation of homogeneous multicellular tumor spheroids applicable to a wide variety of cell types. *Biotechnol. Bioeng.* **83**, 173–180 (2003).
15. Boj, S. F. *et al.* Organoid models of human and mouse ductal pancreatic cancer. *Cell* **160**, 324–338 (2015).
16. Walsh, A. J. *et al.* Quantitative optical imaging of primary tumor organoid metabolism predicts drug response in breast cancer. *Cancer Res.* **74**, 5184–5194 (2014).
17. Francies, H. E., Barthorpe, A., McLaren-Douglas, A., Barendt, W. J. & Garnett, M. J. Drug Sensitivity Assays of Human Cancer Organoid Cultures. *Methods Mol. Biol. Clifton NJ* (2016). doi:10.1007/7651_2016_10
18. Letai, A. Functional precision cancer medicine—moving beyond pure genomics. *Nat. Med.* **23**, 1028–1035 (2017).
19. Tannock, I. F. & Hickman, J. A. Limits to Personalized Cancer Medicine. *N. Engl. J. Med.* **375**, 1289–1294 (2016).
20. Prasad, V., Fojo, T. & Brada, M. Precision oncology: origins, optimism, and potential. *Lancet Oncol.* **17**, e81–e86 (2016).
21. Janzen, D. M. *et al.* An apoptosis-enhancing drug overcomes platinum resistance in a tumour-initiating subpopulation of ovarian cancer. *Nat. Commun.* **6**, (2015).
22. Zhou, Q. Targeting Cyclin-Dependent Kinases in Ovarian Cancer. *Cancer Invest.* **0**, 1–10 (2017).
23. Li, B. *et al.* Therapeutic Rationale to Target Highly Expressed Cdk7 Conferring Poor Outcomes in Triple-Negative Breast Cancer. *Cancer Res.* canres.2546.2016 (2017). doi:10.1158/0008-5472.CAN-16-2546
24. Belmokhtar, C. A., Hillion, J. & Ségal-Bendirdjian, E. Staurosporine induces apoptosis through both caspase-dependent and caspase-independent mechanisms. *Oncogene* **20**, 3354–3362 (2001).
25. Sun, S. *et al.* Prognostic Value and Implication for Chemotherapy Treatment of ABCB1 in Epithelial Ovarian Cancer: A Meta-Analysis. *PLoS ONE* **11**, (2016).
26. Vaidyanathan, A. *et al.* ABCB1 (MDR1) induction defines a common resistance mechanism in paclitaxel- and olaparib-resistant ovarian cancer cells. *Br. J. Cancer* **115**, 431–441 (2016).
27. Huang, L. *et al.* Ductal pancreatic cancer modeling and drug screening using human pluripotent stem cell- and patient-derived tumor organoids. *Nat. Med.* **21**, 1364–1371 (2015).

Methods

Cell lines and primary samples: Cell lines are cultured in their recommended medium in the presence of 10% FBS (Life Technologies #10082-147) and 1% Antibiotic-Antimycotic (Gibco). DU145, PC3, PANC1 and HUTP4 were culture in DMEM (Life Technologies #1195-065). PAN03.27, MDA-MB-468 and MCF-7 was cultured in RPMI (Life Technologies #22400-089). SK-NEP-1 was cultured in McCoy medium (ATCC #30-2007). S1 GODL¹ and S9 GODL² cells are derived from HGSOC primary samples and cultured in RPMI. All treatments are performed in serum-free medium (PrEGM, Lonza #CC-3166).

Primary samples: Primary ovarian cancer specimens were dissociated to single cells and cryopreserved as previously described^{1,2}. In short, fresh tumor specimens or ascites samples are obtained from consented patients (UCLA IRB 10-000727). Solid tumor specimens are minced, then enzymatically digested in 1 mg/ml collagenase and 1 mg/ml dispase. Digested tumors and ascites specimens are then treated with 0.05% Trypsin-EDTA. Trypsinization is stopped with DMEM/10% FBS, and the resulting cell suspension is filtered through a 40 μ M cell strainer. Cells are cryopreserved in 90%FBS/10% DMSO.

Chemicals: Doxorubicin hydrochloride was purchased from Sigma (#44583). Staurosporine was purchased from Cell Signaling Technology (#9953S). ReACp53 was synthesized by GL Biochem and prepared as described³.

3D organoids seeding/treatment procedure: Single-cell suspensions (2K-10K/well) were plated around the rim of the well of 96 well plates in a 3:4 mixture of PrEGM medium and Matrigel (BD Bioscience CB-40324). White plates (Corning #3610) were used for ATP assays while black ones (Corning #3603) were used for caspase or calcein assays. Plates are incubated at 37°C with 5% CO₂ for 15 minutes to solidify the gel before addition of 100 μ l of pre-warmed PrEGM to each well using an EpMotion (Eppendorf). Two days after seeding, medium is removed and replaced with fresh PrEGM containing the indicated drugs. The same procedure is repeated daily on two consecutive days. 24h after the last treatments, media is removed and wells are washed with 100 μ l of pre-warmed PBS. To prepare for downstream experiments, organoids are then released from Matrigel by 40 minutes of incubation in 50 μ l of 5mg/mL dispase (Life Technologies #17105-041). All steps are performed with the EpMotion for small scale experiments and medium is removed/added from the center of the wells. For the high-throughput kinase screening experiment, we utilized a Beckman Coulter Biomek FX system with 96 channel head integrated into a Thermo Spinnaker robotic system with Momentum scheduling software. In short, an intermediary dilution plate (Axygen P-96-450V-C-S) was filled with 100 μ l/well of media and pre-warmed to 37°C. Using pre-sterilized p50 tips, 1 μ l of drug is transferred from a library compound plate to the intermediary media plate and thoroughly mixed. Next, the robot gently removed 100 μ l of media from the matrigel/cell plate. The liquid handler was set up to hit the dead center of each well with no contact to the Matrigel mini-ring. As a last step, the robot transferred 100 μ l from the intermediary plate (media+drug) to the matrigel/cell plate. Media was easily dispensed without touching or disrupting the Matrigel mini-ring. The total process time outside of the CO₂ incubator was less than 2 minutes allowing the temperature to be controlled throughout.

ATP assay: After the organoid release, 75 μ l of Celltiter-Glo 3D Reagent (Promega #G968B) is added to each well followed by 1 minute of vigorous shaking. After a 30 minute incubation at room temperature and an additional minute of shaking, luminescence is measured with a SpectraMax iD3 (Molecular Devices) over 500 ms of integration time. Data is normalized to vehicle and plotted and EC₅₀ values are calculated with Prism 7. For the high-throughput drug screening, DMSO and Staurosporine (1 μ M) are used as negative and positive control respectively. Values are normalized to vehicle. Hits are determined following two criteria: (1) cell death shows concentration-dependency and

(2) residual cell viability at 1 μM is $\leq 25\%$. For Patient #2, partial hits are defined as drugs giving response comparable to Staurosporine (50-60% residual viability at 1 μM).

Caspase 3/7/Hoechst assay: After dispase treatment, 100 μl of Nexcelom ViaStain™ Live Caspase 3/7 staining solution is added to each well. The staining solution consists of 2.5 μM Caspase reagent (Nexcelom #CSK-V0002) and 3 $\mu\text{g/ml}$ Hoechst (Nexcelom #CS1-0128) in serum-free RPMI medium. Plates are incubated 37°C/5% CO₂ for 45 minutes and imaged with a Celigo S Imaging Cell Cytometer (Nexcelom). Data is normalized to vehicle values and plotted with Prism 7.

Calcein-AM/Hoechst/Viability assay: For this assay, 100 μl of Calcein-AM/Hoechst/PI viability staining solution are added to each well containing the released organoids. The staining solution includes the Calcein-AM reagent (Nexcelom CS1 #0119; 1:2000 dilution), Propidium Iodide (Nexcelom #CS1-0116; 1:500 dilution), Hoechst (Nexcelom #CS1-0126; 1:2500 dilution) in serum-free RPMI medium. Samples are incubated for 15 minutes at 37°C with 5% CO₂ before imaging with a Celigo S Imaging Cell Cytometer (Nexcelom).

Immunohistochemistry: Cells processed for fixation were seeded in 24 well plates to facilitate collection. Rings are washed with pre-warmed PBS, followed by 30-minute fixation at room temperature with 4% Formaldehyde EM-Grade (Electron Microscopy Science #15710). Samples are collected in a conical tube and centrifuged at 2000g for 10 minutes at 4°C. Pellets are washed with PBS followed by a second spin. After discarding the supernatant, pellets are mixed in 10 μl of HistoGel (ThermoScientific #HG-40000-012). The mixture is shortly incubated on ice for 5 minutes to solidify the pellets before transferring to a histology cassette for standard embedding and sectioning.

The slides are baked at 45°C for 20 minutes and de-paraffinized in xylene followed by washes in ethanol and D.I. water. Endogenous peroxidases are blocked with Peroxidase-1 (Biocare Medical #PX968M) at RT for 5 minutes. Antigen retrieval is performed in a NxGEN Deloaking Chamber (Biocare Medical) using Diva Decloacker (Biocare Medical #DV2004LX) at 110°C for 15 minutes for Ki-67/Caspase-3 (Biocare Medical #PPM240DSAA) and pTEN (Cell Signaling Technology #CTS 9559) staining or using Borg Decloacker (Biocare Medical #BD1000 S-250) at 90°C for 15 minutes for Anti-P Glycoprotein (Abcam #EPR10364-57) staining. For EGFR staining, antigen retrieval is performed enzymatically with Carezyme III Pronase (Biocare Medical #PRT957) at 37°C for 5 minutes.

Blocking is performed at RT for 30 minutes with 8% Normal Goat Serum (Abcam #AB7841) in TBST for pTEN or using Background Punisher (Biocare Medical #BP947H) at RT for 15 minutes for the EGFR staining. Primary antibodies are diluted in Da Vinci Green Diluent (Biocare Medical #PD900L) for Anti-P Glycoprotein (1:300) and pTEN (1:100) incubated at 4°C overnight or Van Gogh Diluent (Biocare #PD902H) for EGFR (1:30) incubated at RT for 30 minutes. The combo Ki-67/Caspase-3 solution is pre-diluted and added to the sample for 60 minutes at room temperature. Secondary antibody staining is performed with Rabbit on Rodent HRP-polymer (Biocare Medical #RMR622G) for the Anti-P Glycoprotein and pTEN or with Mouse on Mouse HRP-polymer (Biocare Medical #MM620G) for EGFR. MACH 2 double Stain 2 (Biocare Medical #MRCT525G) is used for Ki-67/Caspase-3 combinatorial staining. All secondary antibodies are incubated at RT for 30 minutes.

Chromogen development is performed with Betazoid DAB kit (Biocare Medical #BDB2004) for Anti-P Glycoprotein, pTEN and EGFR and Ki-67 or Warp Red Chromogen Kit (Biocare Medical #WR806) for Caspase-3. The reaction is quenched by dipping the slides in D.I. water. Hematoxylin-1 (Thermo Scientific #7221) is used for counterstaining. The slides are mounted with Permount (Fisher Scientific #SP15-100). Images are acquired with a Revolve Upright and Inverted Microscope System (Echo Laboratories).

Methods References:

1. Janzen, D.M., et al., An apoptosis-enhancing drug overcomes platinum resistance in a tumour-initiating subpopulation of ovarian cancer. *Nat Commun*, 2015. 6: p. 7956.
2. La, V., et al., Birinapant sensitizes platinum resistant carcinomas with high levels of cIAP to carboplatin therapy. *NPJ Precision Oncology*, 2017. In press.
3. Soragni, A. *et al.* A Designed Inhibitor of p53 Aggregation Rescues p53 Tumor Suppression in Ovarian Carcinomas. *Cancer Cell* **29**, 90–103 (2016).

SUPPLEMENTARY MATERIAL

Mini-ring approach for high-throughput drug screenings in 3D tumor models

Nhan Phan, Bobby Tofig, Jessica Huang, Deanna Janzen, Sanaz Memarzadeh, Robert Damoiseaux and Alice Soragni

Supplementary Table:

Stable Lines:		
Specimen	Tumor Classification	Base Medium
MCF7	Invasive breast ductal carcinoma	RPMI
MD-MBA-468	Breast adenocarcinoma	RPMI
PANC1	Pancreatic ductal adenocarcinoma	DMEM
PANC03.27	Pancreatic adenocarcinoma	RPMI
HUPT4	Pancreatic adenocarcinoma	DMEM
PC3	Prostatic adenocarcinoma	DMEM
DU145	Prostatic carcinoma	DMEM
SK-NEP-1	Ewing sarcoma	McCoy
S1 GODL	High-grade serous ovarian carcinoma	RPMI
S9 GODL	High-grade serous ovarian carcinoma	RPMI

Primary Specimens:			
Specimen	Tumor Classification	Sample Type	Therapy
Patient #1	Metastatic clear cell and high grade serous cancer with a 60% clear cell and 40% HGSC component	Ascites	None
Patient #2	High-grade serous ovarian carcinoma, Stage IIIC	Ascites	Carboplatin / Taxol / Avastin

Table S1. Characteristics of samples used in this study.

Supplementary Figures:

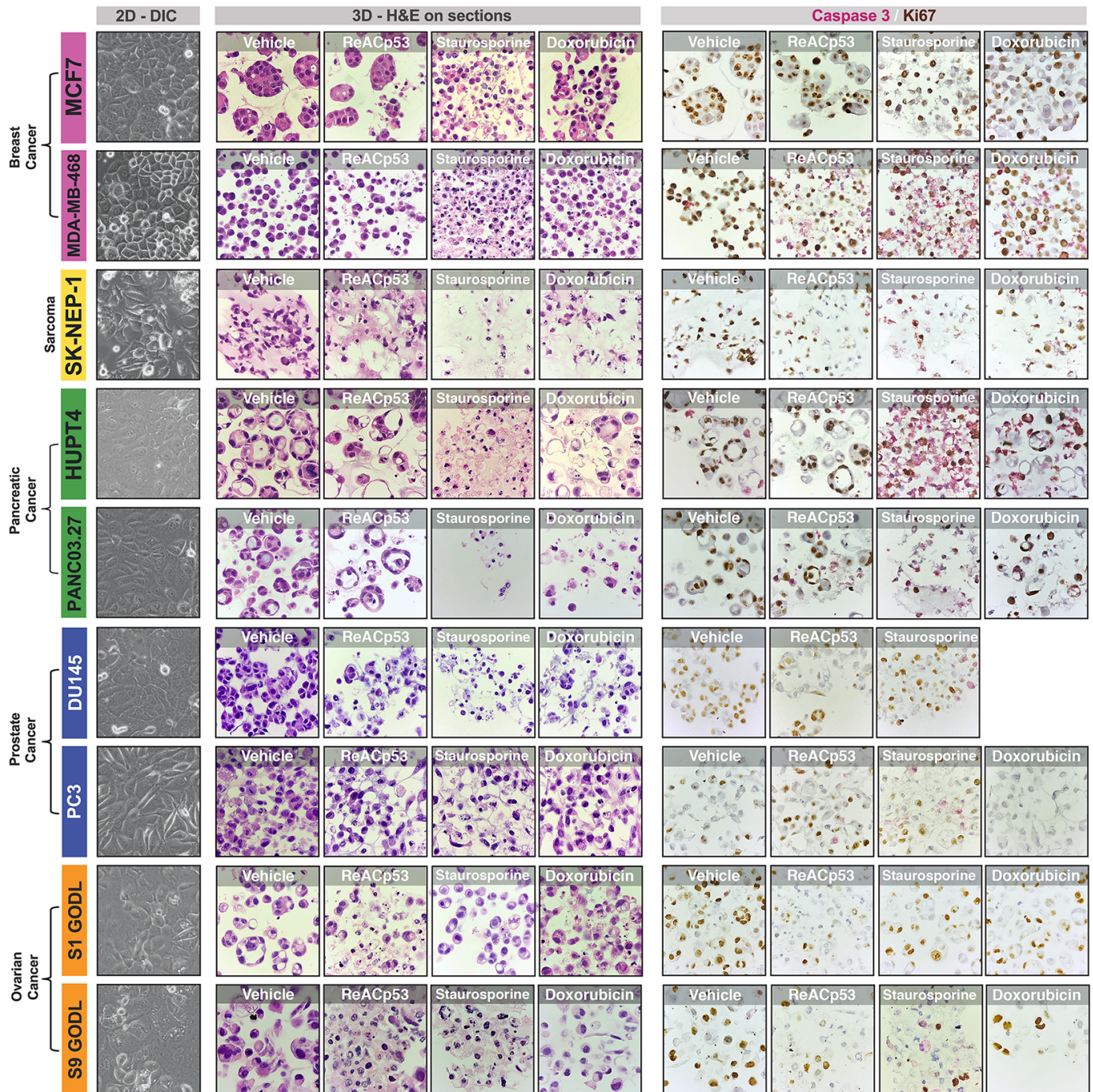
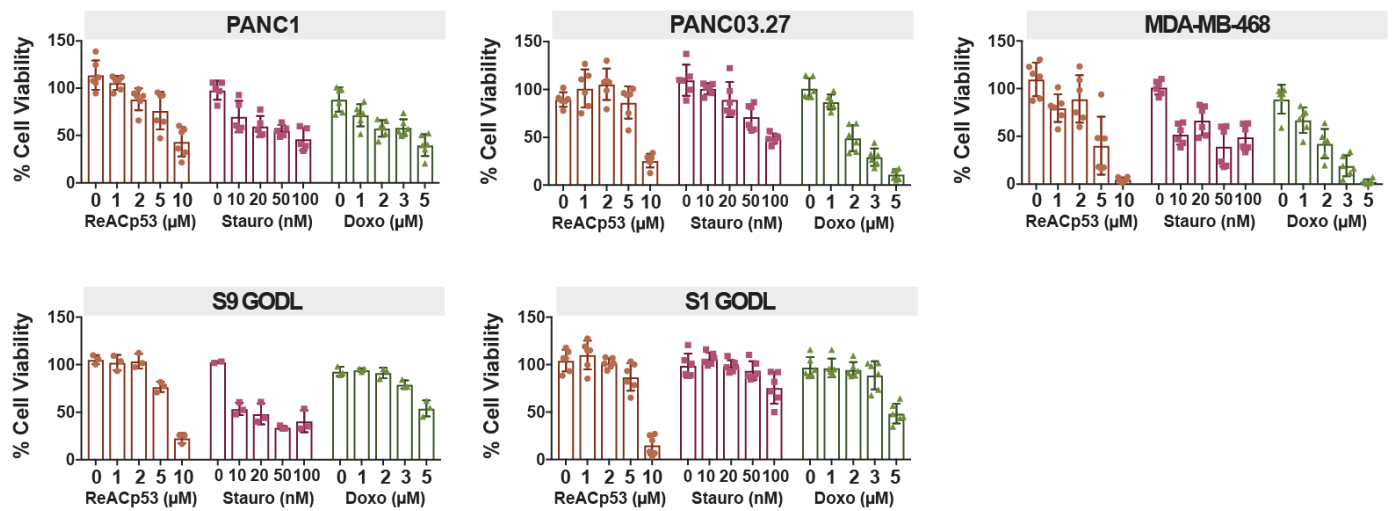


Figure S1. Morphology of 3D tumor models. Tumor cell lines used in this study grown in 3D processed for histology. The corresponding cells grown in 2D are shown on the left (40x magnification). On the right, H&E and Caspase/Ki67 staining on sections from embedded 3D tumor organoid samples (60x magnification).

a



b

	ReACp53	Staurosporin	Doxorubicin
S1 GODL	6.9	0.2	5.0
S9 GODL	7.5	0.2	5.9
SKNEP	2.9	0.3	0.9
MCF7	9.9	0.1	12.0
HUPT4	7.4	0.3	1.5
PANC1	6.9	ND	5.7
PANC03.27	8.5	0.8	2.1
MDA-MB-468	2.5	ND	1.7

Figure S2. ATP readout and EC₅₀ values for three-drug assay. (a) ATP quantification as measured by CellTiter-Glo 3D. Data from 2 independent experiments, n=3 for each are plotted. Error bars represent standard deviation; bars represent mean values. (b) EC₅₀ values as calculate from the ATP quantification data. All values are expressed in μM.

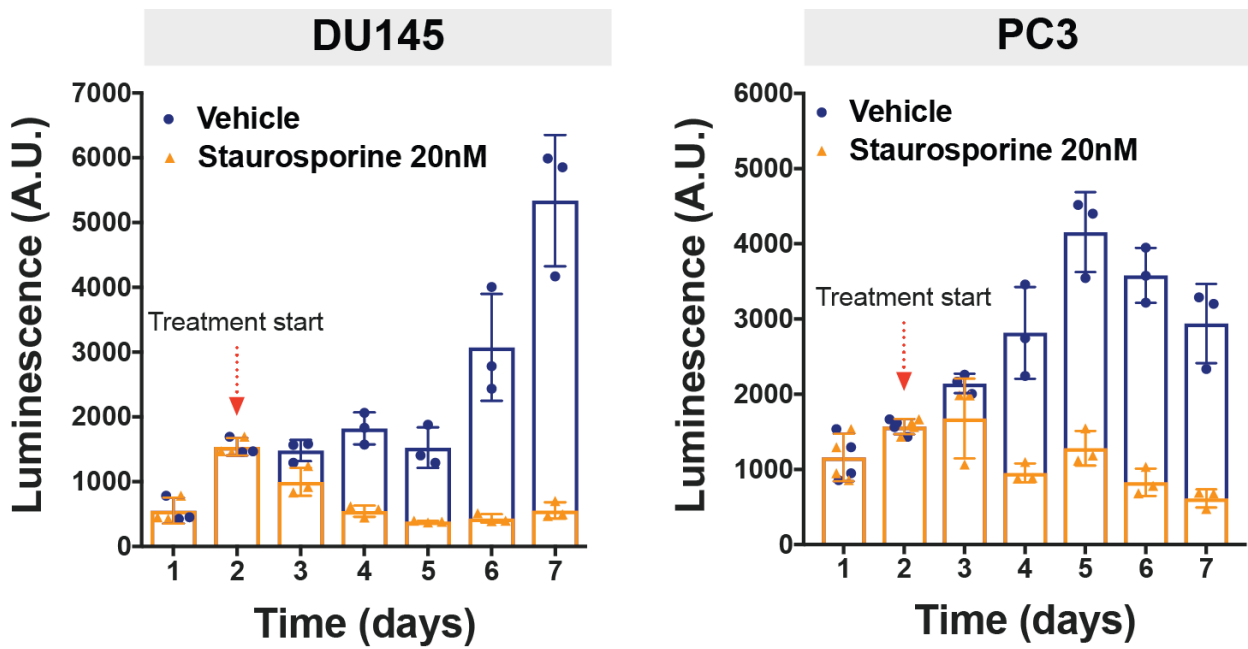


Figure S3. Adaptability of miniring assay to different treatment schedules. ATP quantification as measured by CellTiter-Glo 3D of prostate cancer organoids treated for 5 consecutive days with either vehicle or 20 nM Staurosporine.

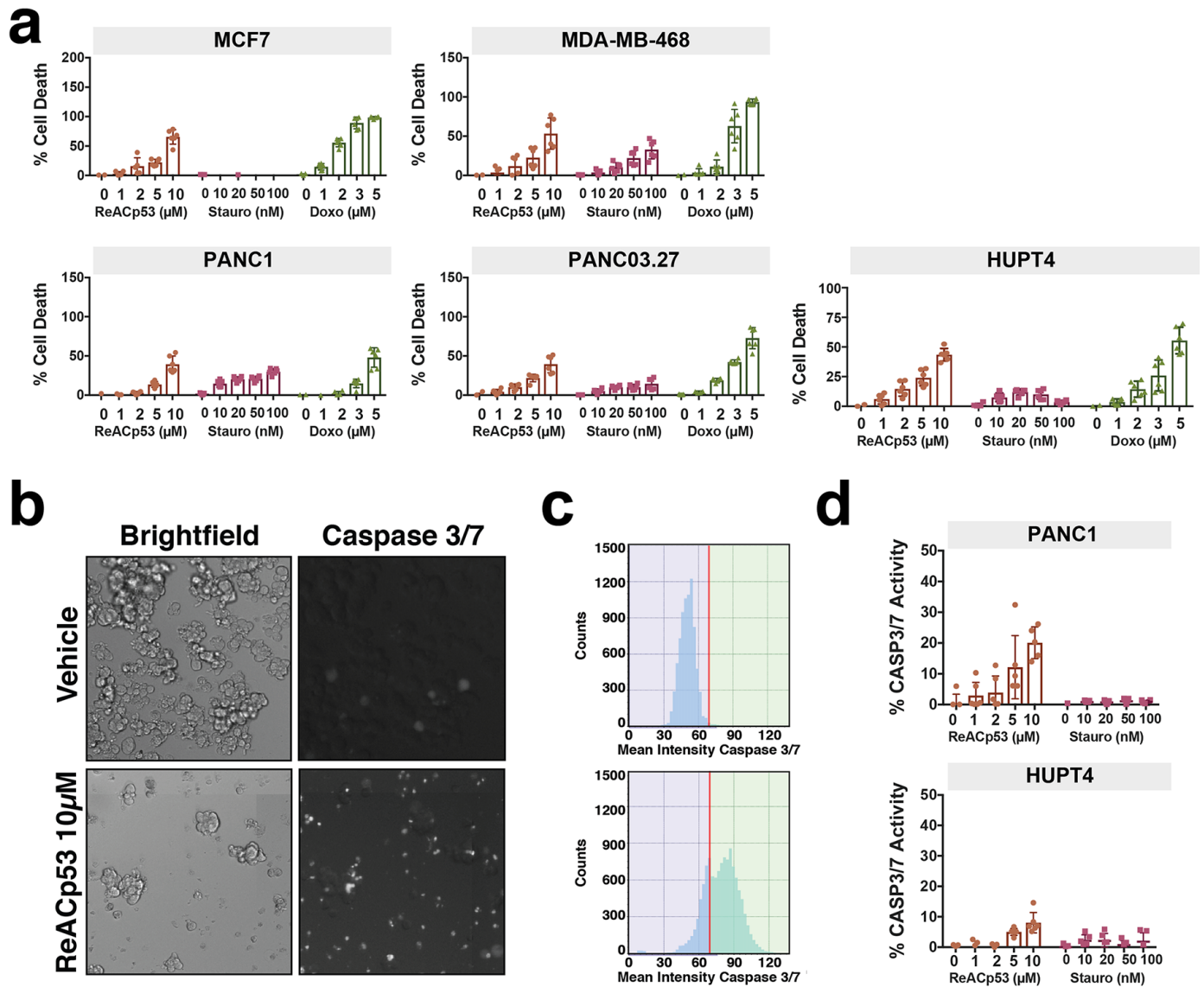


Figure S4. Additional optimized readouts for miniring assay (a) Quantification of the calcein release / PI uptake experiment. Two independent experiments shown, $n=3$ for each. Error bars are standard deviation while bars represent mean values. **(b)** and **(c)** Example of outcome for the caspase 3/7 cleavage experiment. DU145 prostate cancer cells are shown. A substrate becomes fluorescent when cleaved by caspase 3 or 7. Treatment induces high levels of caspase activation. Histograms of fluorescence intensity are shown in **(c)**. **(d)** Quantification of active caspase 3/7 activity normalized to control. Doxorubicin has intrinsic fluorescence that masks the caspase signal hence was excluded from this analysis.

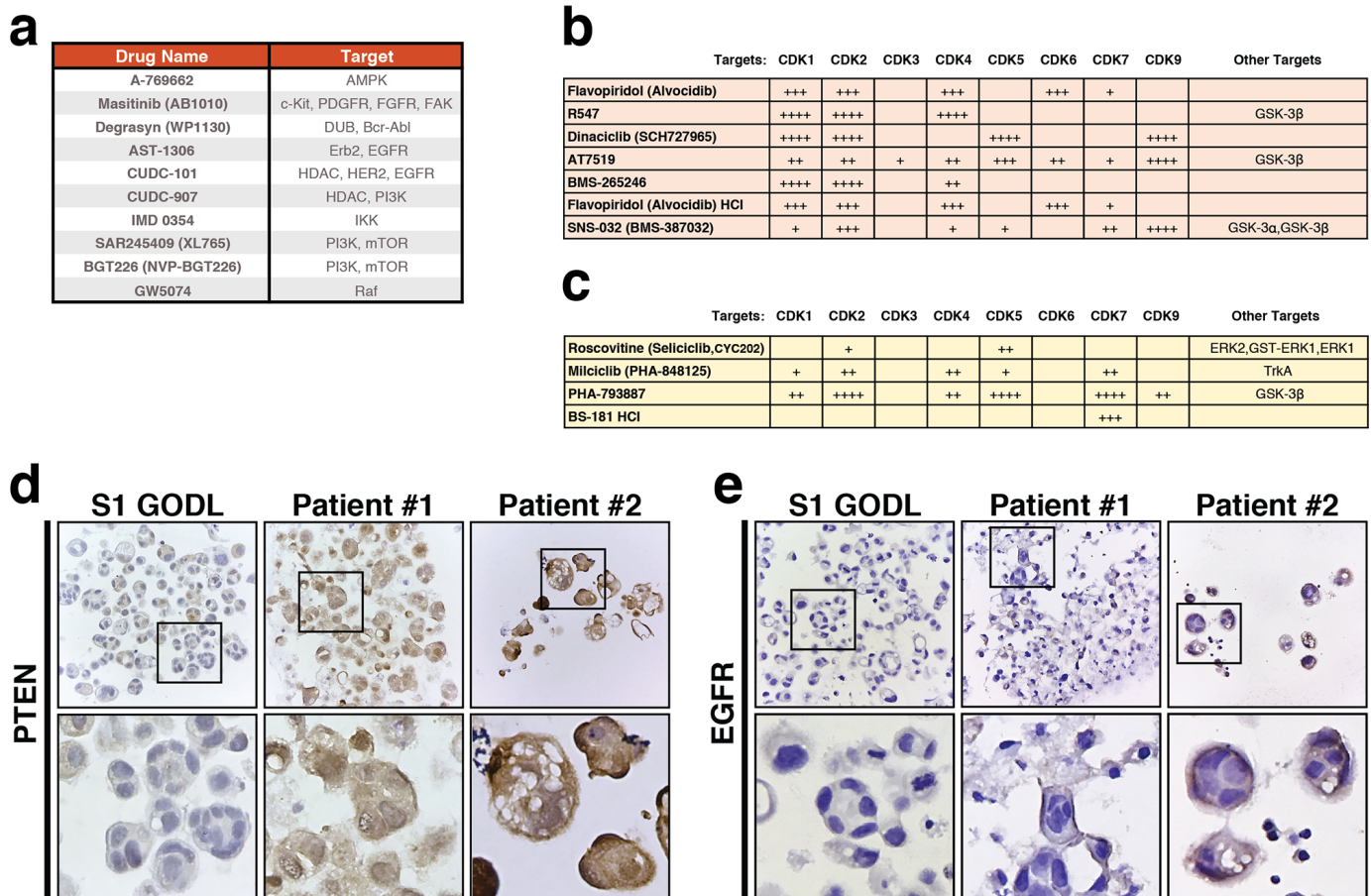


Figure S5. Results and validation of PDO kinase screening. (a) Kinase inhibitors to which the HGSC control patient-derived line S1 GODL responded to. (b) List of CDK inhibitors that induced cell death in >75% Patient #1's organoids. Targets and specificity of each is listed. The patient responded to CDK inhibitors hitting CDK1/2 in combination with CDK 4/6 or CDK 5/9. (c) CDK inhibitors included in the 252-molecule screening that did not induce a response in Patient #1 organoids. The molecules share a low CDK1 targeting activity. (d) PTEN staining of S1 GODL, Patient #1 and Patient #2 organoids. (e) Expression of EGFR in S1 GODL, Patient #1 and Patient #2 3D tumors. Magnification: 40x.